5876 *Inorg. Chem.* **2010**, *49*, 5876–5882
DOI: 10.1021/ic1000717

Inorganic Chemistry
Article

Synthesis, Spectroscopic and Electrochemical Properties, and Electronic Structures of Octahedral Hexatechnetium(III) Clusters $[Tc_6Q_8(CN)_6]^{4-}$ (Q = S, Se)

Takashi Yoshimura,*,† Takuya Ikai,† Tsutomu Takayama,‡ Tsutomu Sekine,§ Yasushi Kino,⊥ and Atsushi Shinohara†

†*Department of Chemistry, Graduate School of Science, Osaka University, Toyonaka, Osaka 560-0043, Japan,* ‡*Department of Chemistry, Daido University, Nagoya, Aichi 457-8530, Japan,* §*Center for the Advancement of Higher Education, Tohoku University, Sendai, Miyagi 980-8576, Japan, and* ⊥*Department of Chemistry, Graduate School of Science, Tohoku University, Sendai, Miyagi 980-8578, Japan*

Received January 13, 2010

Chalcogenide-capped molecular octahedral hexatechnetium(III) clusters $[Tc_6Q_8(CN)_6]^{4-}$ {Q = S ($[\mathbf{1}]^{4-}$), Se ($[\mathbf{2}]^{4-}$)} were prepared by the substitution of axial ligands with cyanide. The structures of the new complexes were determined by single-crystal X-ray analysis. The IR spectra of $[\mathbf{1}]^{4-}$ and $[\mathbf{2}]^{4-}$ showed a C≡N stretching band at 2114 and 2105 cm^{-1}, respectively. In cyclic voltammetry, $[\mathbf{1}]^{4-}$ and $[\mathbf{2}]^{4-}$ in CH_3CN showed reversible one-electron-oxidation waves assignable to the Tc_6(24e/23e) process at +0.99 and +0.74 V, respectively. Density functional theory (DFT) calculations on the hexatechnetium complexes showed that the highest occupied molecular orbital (HOMO) was primarily localized on a Tc_6Q_8 core and the lowest unoccupied molecular orbital (LUMO) was completely localized on the metal orbitals. The energy level of HOMO and the redox potential of the M_6(24e/23e) process (M = Tc, Re) were found to have a good linear relationship. Time-dependent DFT calculations showed that the substantially allowed transitions with the lowest energy were Tc_6Q_8 core-centered transitions. The electronic structures and electronic transition features of the hexatechnetium complexes were similar to those of the hexarhenium analogues $[Re_6Q_8(CN)_6]^{4-}$ (Q = S, Se); however, the energy gap between the HOMO and LUMO was smaller in the hexatechnetium complexes.

Introduction

Among the various polynuclear technetium complexes, the chemistry of technetium−technetium-bonded dinuclear complexes has been studied extensively.[1] In contrast, the chemistry of technetium−technetium-bonded complexes composed of three or more nuclei is still limited.[1a−c,i,2] Most studies on discrete polynuclear technetium−technetium-bonded complexes have dealt with halide-bridged compounds,[1a−c,2f,h] and very little research has been conducted on the other types of complexes. Octahedral hexanuclear cluster complexes are composed of six metal ions that occupy the corners of a nearly regular octahedron with metal−metal single-bond distances, eight face-capping ligands, and six axial ligands (Figure S1 in the Supporting

*To whom correspondence should be addressed. E-mail: tyoshi@chem.sci.osaka-u.ac.jp. Tel.: 81-6-6850-5416. Fax: 81-6-6850-5418.

(1) (a) Sattelberger, A. P. *Multiple Bonds between Metal Atoms*, 3rd ed.; Cotton, F. A., Murillo, C. A., Walton, R. A., Eds.; Springer: Berlin, 2005. (b) Schwochau, K. *Technetium: Chemistry and Radiopharmaceutical Applications*; Wiley-VCH: Weinheim, Germany, 2000; (c) Alberto, R. *Compr. Coord. Chem. II* **2004**, *5*, 127–270. (d) Sattelberger, A. P.; Poineau, F.; Scott, B. L. *Compr. Organomet. Chem. III* **2007**, *5*, 833–854. (e) Poineau, F.; Sattelberger, A. P.; Conradson, S. D.; Czerwinski, K. R. *Inorg. Chem.* **2008**, *47*, 1991–1999. (f) Poineau, F.; Sattelberger, A. P.; Czerwinski, K. R. *J. Coord. Chem.* **2008**, *61*, 2356–2370. (g) Poineau, F.; Gagliardi, L.; Forster, P. M.; Sattelberger, A. P.; Czerwinski, K. R. *Dalton Trans.* **2009**, 5954–5959. (h) Poineau, F.; Weck, P. F.; Forster, P. M.; Sattelberger, A. P.; Czerwinski, K. R. *Dalton Trans.* **2009**, 10338–10342. (i) Poineau, F.; Rodriguez, E. E.; Weck, P. F.; Sattelberger, A. P.; Forster, P.; Hartmann, T.; Mausolf, E.; Silva, G. W. C.; Jarvinen, G. D.; Cheetham, A. K.; Czerwinski, K. R. *J. Radioanal. Nucl. Chem.* **2009**, *282*, 605–609.

(2) (a) Muenze, R. *Radiochem. Radioanal. Lett.* **1981**, *48*, 281–287. (b) Bronger, W.; Kanert, M.; Loevenich, M.; Schmitz, D.; Schwochau, K. *Angew. Chem., Int. Ed. Engl.* **1993**, *32*, 576–578. (c) Bronger, W.; Kanert, M.; Loevenich, M.; Schmitz, D. *Z. Anorg. Allg. Chem.* **1993**, *619*, 2015–2020. (d) Baturin, N. A.; Grigor'ev, M. S.; Kryuchkov, S. V.; Miroslavov, A. E.; Sidorenko, G. V.; Suglobov, D. N. *Radiokhim.* **1994**, *36*, 199–201. (e) Alberto, R.; Schibli, R.; Schubiger, P. A.; Abram, U.; Huebener, R.; Berke, H.; Kaden, T. A. *Chem. Commun.* **1996**, 1291–1292. (f) Kryutchkov, S. V. *Top. Curr. Chem.* **1996**, *176*, 189−252 and references cited therein. (g) Alberto, R.; Schibli, R.; Angst, D.; Schubiger, P. A.; Abram, U.; Abram, S.; Kaden, T. A. *Transition Met. Chem.* **1997**, *22*, 597–601. (h) German, K. E.; Kryutchkov, S. V. *Russ. J. Inorg. Chem.* **2002**, *47*, 578−583 and references cited therein. (i) Lukens, W. W.; Bucher, J. J.; Shuh, D. K.; Edelstein, N. M. *Environ. Sci. Technol.* **2005**, *39*, 8064–8070. (j) Rodriguez, E. E.; Poineau, F.; Llobet, A.; Sattelberger, A. P.; Bhattacharjee, J.; Waghmare, U. V.; Hartmann, T.; Cheetham, A. K. *J. Am. Chem. Soc.* **2007**, *129*, 10244–10248. (k) Poineau, F.; Rodriguez, E. E.; Forster, P. M.; Sattelberger, A. P.; Cheetham, A. K.; Czerwinski, K. R. *J. Am. Chem. Soc.* **2009**, *131*, 910–911. (l) Weck, P. F.; Kim, E.; Poineau, F.; Rodriguez, E. E.; Sattelberger, A. P.; Czerwinski, K. R. *Inorg. Chem.* **2009**, *48*, 6555–6558. (m) Yoshimura, T.; Ikai, T.; Tooyama, Y.; Takayama, T.; Sekine, T.; Kino, Y.; Kirishima, A.; Sato, N.; Mitsugashira, T.; Takahashi, N.; Shinohara, A. *Eur. J. Inorg. Chem.* **2010**, 1214–1219.

 Published on Web 06/02/2010

Information). This type of complex was first synthesized using technetium as Tc_6Q_x (Q = S, Se, $x = 12-14$) by Bronger and colleagues.[2b,c] In a recent study conducted by us, sulfide-capped hexatechnetium(III) halide clusters were obtained as discrete complexes, while selenide- and telluride-capped complexes were obtained as polymeric structures.[2m] However, the chemical properties of octahedral hexatechnetium complexes have still not been elucidated. The redox properties of octahedral hexatechnetium complexes are intriguing because the redox potential of isomorphic hexarhenium complexes can be extensively and precisely controlled by changing the combination of axial and face-capping ligands.[3] It is also of interest to determine whether the octahedral hexatechnetium(III) clusters show photoluminescence because the isoelectronic (24 valence electrons) hexamolybdenum(II), hexatungsten(II), and hexarhenium(III) complexes are strongly luminescent.[3c,f,h,i,l,n,4,5] A large number of cyano-bridged polymeric and supramolecular structures using hexarhenium or hexanuclear rhenium−osmium complexes have been synthesized, and their properties were investigated.[3r,5m,6] Therefore, the chemistry of isostructural and isoelectronic hexatechnetium complexes with axial cyano ligands is of interest in view of its potential application as a building block for supramolecular assemblies.

In this paper, the synthesis, structure, and spectroscopic and electrochemical properties of new hexatechnetium(III) complexes $[Tc_6Q_8(CN)_6]^{4-}$ (Q = S, Se) are reported. A theoretical study of the electronic structures and the electronic transition and vibration energies of these hexatechnetium complexes is also presented. The electronic structure of the hexatechnetium(III) complex is similar to that of the isomorphic hexarhenium(III) complex; however, the energy gap between the highest occupied and lowest unoccupied molecular orbitals (HOMO and LUMO) of the hexatechnetium(III) complex is considerably smaller than that of the hexarhenium(III) complex.

Experimental Section

Materials. The isotope 99-technetium was used to synthesize all of the technetium complexes described in this paper. ***Caution! 99-Technetium is a low-energy β^- emitter ($E_{max} = 290\ keV$) with a half-life of $2.11 \times 10^5 y$.*** $Cs_4[Tc_6S_8Br_6]\cdot CsBr$ and $[Tc_6Se_8I_2]$ were prepared according to the methods available in the literature.[2m] The high-temperature reactions were conducted in silica ampules (i.d. × o.d. × $l = 8 \times 10 \times 100$ mm). Acetonitrile for electrochemistry was distilled over CaH_2 under a N_2 atmosphere. Tetra-*n*-butylammonium hexafluorophosphate (Bu_4NPF_6) as the supporting electrolyte was prepared by metathesis of NH_4PF_6 with Bu_4NBr in H_2O and recrystallized twice from ethanol.

Preparation of the Complexes. $(PPh_4)_4[Tc_6S_8(CN)_6]$ ($(PPh_4)_4$[1]). A mixture of $Cs_4[Tc_6S_8Br_6]\cdot CsBr$ (9.8 mg, 4.7 μmol) and NaCN (4.6 mg, 94 μmol) was placed in a silica ampule, which was then sealed under a static vacuum. The ampule was heated to 640 °C for over 8 h and maintained at 640 °C for 24 h. Thereafter, the ampule was cooled to 300 °C for 12 h and then to room temperature. The reaction mixture was subsequently dissolved in 2 mL of H_2O and then filtered. A solution containing PPh_4Br (40 mg, 95 μmol) in 1 mL of methanol was added to the filtrate. The solid obtained was collected by filtration, washed with methanol and H_2O, and then dried in air. Yield of $(PPh_4)_4$[1]: 6.0 mg (53%). Characterization of the complex was performed using the samples obtained after repeating the aforementioned procedures several times. Anal. Calcd for $(PPh_4)_4$[1]$\cdot 4H_2O$: C, 50.3; H, 3.64. Found: C, 50.3; H, 3.69. IR/cm^{-1} (KBr disk): 2114 ν(C≡N). UV−vis/nm ($\varepsilon/M^{-1}\,cm^{-1}$ in CH_3CN): 425 (1200), 294 (8700), 267 (31 800), 257 (44 400), 224 (sh, 168 000). Single crystals of $(NMe_4)_4$[1]$\cdot 4H_2O$

(3) (a) Gabriel, J. C.; Boubekeur, K.; Batail, P. *Inorg. Chem.* **1993**, *32*, 2894–2900. (b) Zheng, Z.; Holm, R. H. *Inorg. Chem.* **1997**, *36*, 5173–5178. (c) Yoshimura, T.; Ishizaka, S.; Sasaki, Y.; Kim, H.-B.; Kitamura, N.; Naumov, N. G.; Sokolov, M. N.; Fedorov, V. E. *Chem. Lett.* **1999**, 1121–1122. (d) Yoshimura, T.; Umakoshi, K.; Sasaki, Y.; Sykes, A. G. *Inorg. Chem.* **1999**, *38*, 5557–5564. (e) Zheng, Z.; Gray, T. G.; Holm, R. H. *Inorg. Chem.* **1999**, *38*, 4888–4895. (f) Yoshimura, T.; Umakoshi, K.; Sasaki, Y.; Ishizaka, S.; Kim, H.-B.; Kitamura, N. *Inorg. Chem.* **2000**, *39*, 1765–1772. (g) Chen, Z.-N.; Yoshimura, T.; Abe, M.; Sasaki, Y.; Ishizaka, S.; Kim, H.-B.; Kitamura, N. *Angew. Chem., Int. Ed.* **2001**, *40*, 239–242. (h) Chen, Z.-N.; Yoshimura, T.; Abe, M.; Tsuge, K.; Sasaki, Y.; Ishizaka, S.; Kim, H.-B.; Kitamura, N. *Chem.—Eur. J.* **2001**, *7*, 4447–4455. (i) Gabriel, J.-C. P.; Boubekeur, K.; Uriel, S.; Batail, P. *Chem. Rev.* **2001**, *101*, 2037–2066. (j) Tulsky, E. G.; Long, J. R. *Inorg. Chem.* **2001**, *40*, 6990–7002. (k) Roland, B. K.; Carter, C.; Zheng, Z. *J. Am. Chem. Soc.* **2002**, *124*, 6234–6235. (l) Chasse, T. L.; Yohannan, J. C.; Kim, N.; Li, Q.; Li, Z.; Gorman, C. B. *Tetrahedron* **2003**, *59*, 3853–3861. (m) Selby, H. D.; Roland, B. K.; Zheng, Z. *Acc. Chem. Res.* **2003**, *36*, 933–944. (n) Yoshimura, T.; Chen, Z.-N.; Itasaka, A.; Abe, M.; Sasaki, Y.; Ishizaka, S.; Kitamura, N.; Yarovoi, S. S.; Solodovnikov, S. F.; Fedorov, V. E. *Inorg. Chem.* **2003**, *42*, 4857–4863. (o) Roland, B. K.; Flora, W. H.; Carducci, M. D.; Armstrong, N. R.; Zheng, Z. *J. Cluster Sci.* **2004**, *14*, 449–458. (p) Perruchas, S.; Avarvari, N.; Rondeau, D.; Levillain, E.; Batail, P. *Inorg. Chem.* **2005**, *44*, 3459–3465. (q) Roland, B. K.; Flora, W. H.; Armstrong, N. R.; Zheng, Z. *C. R. Chim.* **2005**, *8*, 1798–1807. (r) Welch, E. J.; Long, J. R. In *Progress in Inorganic Chemistry*; John Wiley & Sons, Inc.: New York , 2005; Vol. *54*, pp 1−45. (s) Roland, B. K.; Flora, W. H.; Selby, H. D.; Armstrong, N. R.; Zheng, Z. *J. Am. Chem. Soc.* **2006**, *128*, 6620–6625.

(4) (a) Gray, H. B.; Maverick, A. W. *Science* **1981**, *214*, 1201–1205. (b) Maverick, A. W.; Gray, H. B. *J. Am. Chem. Soc.* **1981**, *103*, 1298–1300. (c) Maverick, A. W.; Najdzionek, J. S.; MacKenzie, D.; Nocera, D. G.; Gray, H. B. *J. Am. Chem. Soc.* **1983**, *105*, 1878–1882. (d) Zietlow, T. C.; Hopkins, M. D.; Gray, H. B. *J. Solid State Chem.* **1985**, *57*, 112–119. (e) Zietlow, T. C.; Nocera, D. G.; Gray, H. B. *Inorg. Chem.* **1986**, *25*, 1351–1353. (f) Jackson, J. A.; Turro, C.; Newsham, M. D.; Nocera, D. G. *J. Phys. Chem.* **1990**, *94*, 4500–4507. (g) Szczepura, L. F.; Ketcham, K. A.; Ooro, B. A.; Edwards, J. A.; Templeton, J. N.; Cedeno, D. L.; Jircitano, A. J. *Inorg. Chem.* **2008**, *47*, 7271–7278. (h) Gray, T. G. *Chem.—Eur. J.* **2009**, *15*, 2581–2593. (i) Szczepura, L. F.; Edwards, J. A.; Cedeno, D. L. *J. Cluster Sci.* **2009**, *20*, 105–112.

(5) (a) Gray, T. G.; Rudzinski, C. M.; Nocera, D. G.; Holm, R. H. *Inorg. Chem.* **1999**, *38*, 5932–5933. (b) Guilbaud, C.; Deluzet, A.; Domercq, B.; Molinie, P.; Boubekeur, K.; Batail, P.; Coulon, C. *Chem. Commun.* **1999**, 1867–1868. (c) Yoshimura, T.; Ishizaka, S.; Umakoshi, K.; Sasaki, Y.; Kim, H.-B.; Kitamura, N. *Chem. Lett.* **1999**, 697–698. (d) Gray, T. G.; Rudzinski, C. M.; Meyer, E. E.; Holm, R. H.; Nocera, D. G. *J. Am. Chem. Soc.* **2003**, *125*, 4755–4770. (e) Gray, T. G.; Rudzinski, C. M.; Meyer, E. E.; Nocera, D. G. *J. Phys. Chem. A* **2004**, *108*, 3238–3243. (f) Kitamura, N.; Ueda, Y.; Ishizaka, S.; Yamada, K.; Aniya, M.; Sasaki, Y. *Inorg. Chem.* **2005**, *44*, 6308–6313. (g) Mironov, Y. V.; Shestopalov, M. A.; Brylev, K. A.; Yarovoi, S. S.; Romanenko, G. V.; Fedorov, V. E.; Spies, H.; Pietzsch, H.-J.; Stephan, H.; Geipel, G.; Bernhard, G.; Kraus, W. *Eur. J. Inorg. Chem.* **2005**, 657–661. (h) Sasaki, Y. *J. Nucl. Radiochem. Sci.* **2005**, *6*, 145–148. (i) Yarovoi, S. S.; Mironov, Y. V.; Naumov, D. Y.; Gatilov, Y. V.; Kozlova, S. G.; Kim, S.-J.; Fedorov, V. E. *Eur. J. Inorg. Chem.* **2005**, 3945–3949. (j) Mironov, Y. V.; Brylev, K. A.; Shestopalov, M. A.; Yarovoi, S. S.; Fedorov, V. E.; Spies, H.; Pietzsch, H.-J.; Stephan, H.; Geipel, G.; Bernhard, G.; Kraus, W. *Inorg. Chim. Acta* **2006**, *359*, 1129–1134. (k) Sasaki, Y. *Bull. Jpn. Soc. Coord. Chem.* **2006**, *48*, 50–58. (l) Brylev, K. A.; Mironov, Y. V.; Yarovoi, S. S.; Naumov, N. G.; Fedorov, V. E.; Kim, S.-J.; Kitamura, N.; Kuwahara, Y.; Yamada, K.; Ishizaka, S.; Sasaki, Y. *Inorg. Chem.* **2007**, *46*, 7414–7422. (m) Kim, S.; Kim, Y.; Lee, J.; Shin, W.; Lee, M.; Kim, S.-J. *Inorg. Chim. Acta* **2007**, *360*, 1890–1894. (n) Shestopalov, M. A.; Mironov, Y. V.; Brylev, K. A.; Kozlova, S. G.; Fedorov, V. E.; Spies, H.; Pietzsch, H.-J.; Stephan, H.; Geipel, G.; Bernhard, G. *J. Am. Chem. Soc.* **2007**, *129*, 3714–3721. (o) Shestopalov, M. A.; Mironov, Y. V.; Brylev, K. A.; Fedorov, V. E. *Russ. Chem. Bull.* **2008**, *57*, 1644–1649. (p) Brylev, K. A.; Mironov, Y. V.; Kozlova, S. G.; Fedorov, V. E.; Kim, S.-J.; Pietzsch, H.-J.; Stephan, H.; Ito, A.; Ishizaka, S.; Kitamura, N. *Inorg. Chem.* **2009**, *48*, 2309–2315. (q) Dorson, F.; Molard, Y.; Cordier, S.; Fabre, B.; Efremova, O.; Rondeau, D.; Mironov, Y.; Circu, V.; Naumov, N.; Perrin, C. *Dalton Trans.* **2009**, 1297–1299. (r) Shestopalov, M. A.; Cordier, S.; Hernandez, O.; Molard, Y.; Perrin, C.; Perrin, A.; Fedorov, V. E.; Mironov, Y. V. *Inorg. Chem.* **2009**, *48*, 1482–1489. (s) Yoshimura, T.; Suo, C.; Tsuge, K.; Ishizaka, S.; Nozaki, K.; Sasaki, Y.; Kitamura, N.; Shinohara, A. *Inorg. Chem.* **2010**, *49*, 531–540. (t) Yoshimura, T.; Matsuda, A.; Ito, Y.; Ishizaka, S.; Shinoda, S.; Tsukube, H.; Kitamura, N.; Shinohara, A. *Inorg. Chem.* **2010**, *49*, 3473–3481.

were obtained by the slow evaporation of an aqueous solution of the reaction mixture containing NMe_4Br instead of PPh_4Br.

$(PPh_4)_4[Tc_6Se_8(CN)_6]$ ($(PPh_4)_4$[2]). A mixture of $[Tc_6Se_8I_2]$ (13.9 mg, 9.40 μmol) and NaCN (9.2 mg, 190 μmol) was placed in a silica ampule, which was then sealed under a static vacuum. The ampule was heated to 640 °C for over 8 h and maintained at 640 °C for 24 h. The sample was then cooled to 300 °C for 12 h and then to room temperature. The reaction mixture was dissolved in 2 mL of H_2O and then filtered. A solution containing PPh_4Br (20 mg, 48 μmol) in 1 mL of methanol was added to the filtrate. The solid obtained was collected by filtration, washed with methanol and H_2O, and then dried in air. Yield of $(PPh_4)_4$[2]: 19.9 mg (77%). Anal. Calcd for $(PPh_4)_4$[2]·$3H_2O$: C, 43.9; H, 3.10. Found: C, 43.8; H, 3.20. IR/cm^{-1} (KBr disk): 2105 ν(C≡N). UV−vis/nm (ε/M^{-1} cm^{-1} in CH_3CN): 443 (1200), 314 (sh, 7400), 275 (31 000), 268 (30 500), 224 (sh, 160 000). Single crystals of $(PPh_4)_4$[2]·$2CH_3CN$ were obtained from the CH_3CN/diisopropyl ether layer, and those of $(NMe_4)_4$[2]·$2.67H_2O$ were obtained by slow diffusion of an aqueous solution containing NMe_4Br instead of PPh_4Br.

X-ray Crystallographic Determinations. Single crystals of $(NMe_4)_4$[1]·$4H_2O$, $(NMe_4)_4$[2]·$2.67H_2O$, and $(PPh_4)_4$[2]·$2CH_3CN$ were sealed in three separate thin-walled glass capillaries. X-ray crystallographic data for $(NMe_4)_4$[1]·$4H_2O$ and $(NMe_4)_4$[2]·$2.67H_2O$ were collected using a Rigaku RAXIS RAPID detector at 296 K by a standard strategy. X-ray crystallographic data for $(PPh_4)_4$[2]·$2CH_3CN$ were collected using a Rigaku AFC 7R diffractometer at 296 K. The crystal structures were solved by the Patterson method or direct methods. Atomic coordinates and thermal parameters of non-hydrogen atoms were calculated by a full-matrix least-squares method. The hydrogen atoms were included in the calculated positions, except for those of the H_2O molecules. Calculations were performed using *TEXSAN*.[7] The crystallographic data are summarized in Table 1.

Measurements. UV−vis spectra were recorded on a Jasco V-550 spectrophotometer. Elemental analysis was performed using a Yanaco MT-3 analyzer. IR spectra were recorded on a Perkin-Elmer 983G spectrophotometer. Cyclic voltammetry (CV) measurements were performed on a potentiostat (Hokuto Denko, HABF 1510 m) with an $X-Y$ recorder at room temperature using a scan rate of 100 mV s^{-1}. A glassy carbon disk (diameter = 1 mm) and a platinum wire were used as the working and counter electrodes, respectively. A solution of the sample (1 mM) in 0.1 M $Bu_4NPF_6-CH_3CN$ was deoxygenated by an Ar stream. An Ag/AgCl electrode was used as the reference electrode. The half-wave potential of ferrocene/ferrocenium (Fc/Fc^+) at +0.43 V in 0.1 M $Bu_4NPF_6-CH_3CN$ was used as the internal standard.

Computational Methods. Density functional theory (DFT) calculations of $[M_6Q_8(CN)_6]^{4-}$ (M = Tc, Re; Q = S, Se) were performed with the *Gaussian 03* program at the B3LYP level using a LANL2DZ basis set.[8] The model compounds were assumed to have idealized O_h structures with average atomic distances and angles found in $[M_6Q_8(CN)_6]^{4-}$. The geometry of each complex was optimized, and the potential minimum was confirmed on the basis of the result that all of the calculated vibrational frequencies were positive. Single-point DFT and time-dependent DFT (TD-DFT) calculations were performed using optimized geometries. The energies and components of the MOs near the frontier orbital levels were calculated (given in the Supporting Information). The contour plots of the MOs were generated using *GaussView 3.0* software.[9]

Results and Discussion

Preparation and Characterization of the Complexes. Cyanide is one of the well-known depolymerization reagents for polymeric octahedral hexanuclear clusters. The high-temperature method used to substitute the axial ligand in polymeric and discrete octahedral hexanuclear complexes with cyanide was applied to hexarhenium,[3r,6a,h,af,10] hexamolybdenum,[10k,11] hexaniobium,[12] and mixed rhenium−molybdenum clusters[13] at temperatures

(6) (a) Beauvais, L. G.; Shores, M. P.; Long, J. R. *Chem. Mater.* **1998**, *10*, 3783–3786. (b) Naumov, N. G.; Virovets, A. V.; Sokolov, M. N.; Artemkina, S. B.; Fedorov, V. E. *Angew. Chem., Int. Ed.* **1998**, *37*, 1943–1945. (c) Shores, M. P.; Beauvais, L. G.; Long, J. R. *Inorg. Chem.* **1999**, *38*, 1648–1649. (d) Shores, M. P.; Beauvais, L. G.; Long, J. R. *J. Am. Chem. Soc.* **1999**, *121*, 775–779. (e) Beauvais, L. G.; Shores, M. P.; Long, J. R. *J. Am. Chem. Soc.* **2000**, *122*, 2763–2772. (f) Bennett, M. V.; Shores, M. P.; Beauvais, L. G.; Long, J. R. *J. Am. Chem. Soc.* **2000**, *122*, 6664–6668. (g) Naumov, N. G.; Virovets, A. V.; Fedorov, V. E. *Inorg. Chem. Commun.* **2000**, *3*, 71–72. (h) Naumov, N. G.; Virovets, A. V.; Fedorov, V. E. *J. Struct. Chem.* **2000**, *41*, 499–520. (i) Bennett, M. V.; Beauvais, L. G.; Shores, M. P.; Long, J. R. *J. Am. Chem. Soc.* **2001**, *123*, 8022–8032. (j) Kim, Y.; Park, S.-M.; Nam, W.; Kim, S.-J. *Chem. Commun.* **2001**, 1470–1471. (k) Mironov, Y. V.; Fedorov, V. E.; Ijjaali, I.; Ibers, J. A. *Inorg. Chem.* **2001**, *40*, 6320–6323. (l) Naumov, N. G.; Artemkina, S. B.; Fedorov, V. E.; Soldatov, D. V.; Ripmeester, J. A. *Chem. Commun.* **2001**, 571–572. (m) Fedorov, V. E.; Naumov, N. G.; Mironov, Y. V.; Virovets, A. V.; Artemkina, S. B.; Brylev, K. A.; Yarovoi, S. S.; Efremova, O. A.; Peak, U. H. *J. Struct. Chem.* **2002**, *43*, 669–684. (n) Kim, Y.; Park, S.-M.; Kim, S.-J. *Inorg. Chem. Commun.* **2002**, *5*, 592–595. (o) Kim, Y.; Choi, S. K.; Park, S.-M.; Nam, W.; Kim, S.-J. *Inorg. Chem. Commun.* **2002**, *5*, 612–615. (p) Brylev, K. A.; Naumov, N. G.; Peris, G.; Llusar, R.; Fedorov, V. E. *Polyhedron* **2003**, *22*, 3383–3387. (q) Park, S.-m.; Kim, Y.; Kim, S.-j. *Eur. J. Inorg. Chem.* **2003**, 4117–4121. (r) Tulsky, E. G.; Crawford, N. R. M.; Baudron, S. A.; Batail, P.; Long, J. R. *J. Am. Chem. Soc.* **2003**, *125*, 15543–15553. (s) Brylev, K. A.; Mironov, Y. V.; Naumov, N. G.; Fedorov, V. E.; Ibers, J. A. *Inorg. Chem.* **2004**, *43*, 4833–4838. (t) Brylev, K. A.; Sekar, P.; Naumov, N. G.; Fedorov, V. E.; Ibers, J. A. *Inorg. Chim. Acta* **2004**, *357*, 728–732. (u) Kim, Y.; Kim, S.; Kim, S.-J.; Lee, M. K.; Kim, M.; Lee, H.; Chin, C. S. *Chem. Commun.* **2004**, 1692–1693. (v) Mironov, Y. V.; Naumov, N. G.; Brylev, K. A.; Efremova, O. A.; Fedorov, V. E.; Hegetschweiler, K. *Angew. Chem., Int. Ed.* **2004**, *43*, 1297–1300. (w) Naumov, N. G.; Virovets, A. V.; Artemkina, S. B.; Naumov, D. Y.; Howard, J. A. K.; Fedorov, V. E. *J. Solid State Chem.* **2004**, *177*, 1896–1904. (x) Brylev, K. A.; Pilet, G.; Naumov, N. G.; Perrin, A.; Fedorov, V. E. *Eur. J. Inorg. Chem.* **2005**, 461–466. (y) Brylev, K. A.; Naumov, N. G.; Fedorov, V. E.; Ibers, J. A. *J. Struct. Chem.* **2005**, *46*, S130–S136. (z) Naumov, N. G.; Tarasenko, M. S.; Virovets, A. V.; Kim, Y.; Kim, S.-J.; Fedorov, V. E. *Eur. J. Inorg. Chem.* **2006**, 298–303. (aa) Artemkina, S. B.; Naumov, N. G.; Mironov, Y. V.; Sheldrick, W. S.; Virovets, A. V.; Fenske, D. *Russ. J. Coord. Chem.* **2007**, *33*, 867–875. (ab) Xu, L.; Kim, Y.; Kim, S.-J.; Kim, H. J.; Kim, C. *Inorg. Chem. Commun.* **2007**, *10*, 586–589. (ac) Suh, M.-J.; Vien, V.; Huh, S.; Kim, Y.; Kim, S.-J. *Eur. J. Inorg. Chem.* **2008**, 686–692. (ad) Brylev, K. A.; Mironov, Y. V.; Fedorov, V. E. *J. Struct. Chem.* **2009**, *50*, 1197–1200. (ae) Huh, S.; Suh, M.-J.; Vien, V.; Kim, Y.; Hwang, S.-J.; Kim, S.-J. *Small* **2009**, *5*, 1123–1127. (af) Kim, Y.; Fedorov, V. E.; Kim, S.-J. *J. Mater. Chem.* **2009**, *19*, 7178–7190. (ag) Vien, V.; Suh, M.-J.; Huh, S.; Kim, Y.; Kim, S.-J. *Chem. Commun.* **2009**, 541–543.

(7) *TEXSAN*; Molecular Structure Corp.: The Woodlands, TX, 1985 and 1992.

(8) (a) Becke, A. D. *Phys. Rev. B* **1988**, *38*, 3098–3100. (b) Becke, A. D. *J. Chem. Phys.* **1993**, *98*, 4648–5652. (c) Lee, C.; Yang, W.; Parr, R. G. *Phys. Rev. B* **1988**, *37*, 785–789. (d) Frisch, M. J.; Trucks, G. W.; Schlegel, H. B.; Scuseria, G. E.; Robb, M. A.; Cheeseman, J. R.; Montgomery, J., J. A.; Vreven, T.; Kudin, K. N.; Burant, J. C. et al. *Gaussian 03*, revision C.02; Gaussian, Inc.: Wallingford, CT, 2004.

(9) Dennington, R. V., II; Keith, T.; Millam, J.; Eppinnett, K.; Hovell, W. L.; Gilliland, R.; *GaussView*; Semichem, Inc.: Shawnee Mission, KS, 2003.

(10) (a) Mironov, Y. V.; Virovets, A. V.; Fedorov, V. E.; Podberezskaya, N. V. *Polyhedron* **1995**, *14*, 3171–3173. (b) Slougui, A.; Mironov, Y. V.; Perrin, A.; Fedorov, V. E. *Croat. Chem. Acta* **1995**, *68*, 885–890. (c) Mironov, Y. V.; Cody, J. A.; Albrecht-Schmitt, T. E.; Ibers, J. A. *J. Am. Chem. Soc.* **1997**, *119*, 493–498. (d) Imoto, H.; Naumov, N. G.; Virovets, A. V.; Saito, T.; Fedorov, V. E. *J. Struct. Chem.* **1998**, *39*, 720–727. (e) Naumov, N. G.; Virovets, A. V.; Podberezskaya, N. V.; Fedorov, V. E. *J. Struct. Chem.* **1998**, *38*, 857–862. (f) Mironov, Y. V.; Fedorov, V. E.; McLauchlan, C. C.; Ibers, J. A. *Inorg. Chem.* **2000**, *39*, 1809–1811. (g) Artemkina, S. B.; Naumov, N. G.; Virovets, A. V.; Fedorov, V. E. *J. Struct. Chem.* **2002**, *43*, 689–693. (h) Gray, T. G. *Coord. Chem. Rev.* **2003**, *243*, 213–235. (i) Pilet, G.; Perrin, A. *C. R. Chim.* **2005**, *8*, 1728–1742. (j) Naumov, N. G.; Kim, S. J.; Virovets, A. V.; Mironov, Y. V.; Fedorov, V. E. *Bull. Korean Chem. Soc.* **2006**, *27*, 635–636. (k) Fedorov, V. E.; Mironov, Y. V.; Naumov, N. G.; Sokolov, M. N.; Fedin, V. P. *Russ. Chem. Rev.* **2007**, *76*, 529–552.

Table 1. Crystallographic Data for $(NMe_4)_4$[**1**]·$4H_2O$, $(NMe_4)_4$[**2**]·$2.67H_2O$, and $(PPh_4)_4$[**2**]·$2CH_3CN$

	$(NMe_4)_4$[**1**]·$4H_2O$	$(NMe_4)_4$[**2**]·$2.67H_2O$	$(PPh_4)_4$[**2**]·$2CH_3CN$
formula	$C_{22}H_{48}N_{10}O_4S_8Tc_6$	$C_{66}H_{96}N_{30}O_{28}Tc_{18}Se_{24}$	$C_{106}H_{86}N_8P_4Se_8Tc_6$
fw	1367.22	5114.72	2809.47
cryst syst	monoclinic	monoclinic	triclinic
space group	$C2/c$	$P2_1/n$	$P\bar{1}$
a/Å	20.191(7)	11.41(1)	13.159(2)
b/Å	11.659(4)	32.55(2)	16.940(3)
c/Å	23.201(7)	20.29(2)	12.616(2)
α/deg			84.00(2)
β/deg	112.00(1)	101.40(4)	101.42(1)
γ/deg			70.48(1)
V/Å^3	5063(3)	7387(9)	2553.4(8)
Z	4	2	1
D/g cm^{-3}	1.793	2.283	1.827
T/K	296.2	296.2	296.2
μ/cm^{-1}	1.941	7.566	3.747
R_1	0.046	0.048	0.060
R_w	0.161	0.092	0.213
GOF	1.09	1.13	0.88

greater than 600 °C and to mixed rhenium−osmium complexes in $NaCN/NaNO_3$ or $NaCN/KCF_3SO_3$ at 320 or 330 °C.[3r,6r] This procedure was applied to obtain a molecular hexatechnetium complex with axial cyano ligands. Sulfide- and selenide-capped hexatechnetium(III) clusters $[Tc_6Q_8(CN)_6]^{4-}$ ([**1**]$^{4-}$, Q = S; [**2**]$^{4-}$, Q = Se) were prepared by the high-temperature reaction of a discrete molecule (Q = S) and a polymeric complex (Q = Se) with excess sodium cyanide. Each reaction product was dissolved in H_2O, and then PPh_4Br was added to the solution; a yellow-orange complex was obtained. The structures of the complexes were determined by single-crystal X-ray analysis (vide infra). As shown in the IR spectra of [**1**]$^{4-}$ and [**2**]$^{4-}$ (Figures S2 and S3 in the Supporting Information, respectively), a C≡N stretching band was observed at 2114 and 2105 cm^{-1}, respectively. These findings indicate that complexes with cyano ligands have idealized O_h symmetry. The C≡N stretching bands of both hexatechnetium complexes were observed at frequencies similar to those of the hexarhenium analogues ($M_4[Re_6S_8(CN)_6]$, 2105 and 2129 cm^{-1} (M_4 = Cs_3Na),[6a] 2119 cm^{-1} (M_4 = Cs_3K);[14] $M_4[Re_6Se_8(CN)_6]$, 2108 cm^{-1} (M = NMe_4),[10c] 2092 and 2116 cm^{-1} (M_4 = Cs_3Na),[6a] 2107 cm^{-1} (M = K).[10e]

The UV−vis absorption spectra of the new hexatechnetium(III) clusters, $(PPh_4)_4$[**1**] and $(PPh_4)_4$[**2**], were recorded in CH_3CN at room temperature. In the spectrum of [**1**]$^{4-}$, strong absorption bands observed for $[Tc_6S_8Br_6]^{4-}$ at 344 and 320 nm were not present, but new peaks were observed at 425 and 294 nm. The spectral features of [**1**]$^{4-}$ and [**2**]$^{4-}$ resembled each other, but the absorption peaks of the selenide-capped complex [**2**]$^{4-}$ at 443 and 314 nm were at a somewhat longer wavelength than those of the sulfide complex. It is noted that the absorption spectral features of [**1**]$^{4-}$ and [**2**]$^{4-}$ resemble those of the hexarhenium analogues. A longer-wavelength shift of the absorption peak maximum for the selenide-capped complex than for the sulfide-capped analogue was also observed in $[Re_6Q_8(CN)_6]^{4-}$ (Q = S, Se). The assignment of the absorption peak at 425 nm for [**1**]$^{4-}$ and 443 nm for [**2**]$^{4-}$ is discussed in detail in the HOMO and LUMO Properties section.

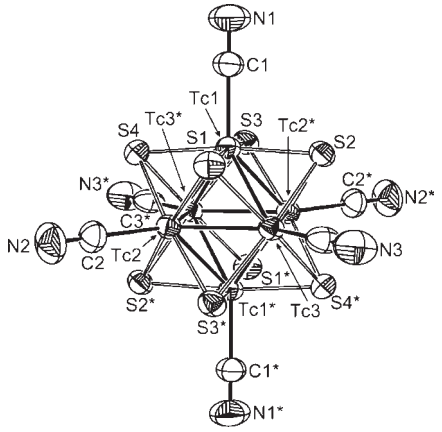

Figure 1. ORTEP drawing showing the complex anion and numbering scheme for $(NMe_4)_4$[**1**].

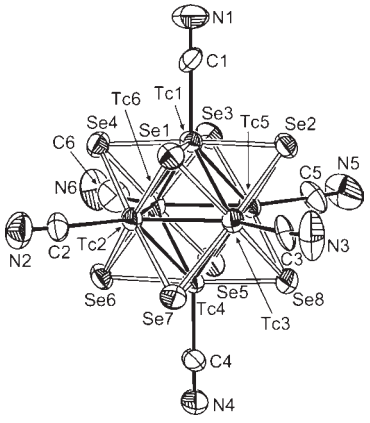

Figure 2. ORTEP drawing showing the complex anion and numbering scheme for $(NMe_4)_4$[**2**].

Crystal Structures of the Complexes. The crystal structures of [**1**]$^{4-}$ and [**2**]$^{4-}$ are shown in Figures 1 and 2, respectively. The selected bond distances and angles are listed in Table 2. The overall structures of the complex anions [**2**]$^{4-}$ in both the NMe_4 and PPh_4 salts are very similar; thus, the structure of the NMe_4 salt is discussed below. In [**1**]$^{4-}$ and [**2**]$^{4-}$, the six technetium atoms form an octahedron with Tc−Tc−Tc angles of 59.78(2)−60.25(2)° and 89.78(2)−90.22(2)° for [**1**]$^{4-}$ and 59.73(4)−60.29(4)° and 89.79(4)−90.38(4)° for [**2**]$^{4-}$. The eight chalcogenides capping the metal triangle face Tc−Q−Tc = av. 65.5(2)° for [**1**]$^{4-}$ and av. 63.3(3)° for [**2**]$^{4-}$ and are arranged at the vertex positions of a cube with Q−Tc−Q angles of av. 89.82(2)° and av. 173.21(1)° for [**1**]$^{4-}$ and av. 89.9(3)° and av. 175.9(3)° for [**2**]$^{4-}$. The Tc−Q−Tc angles in the case of selenium are slightly smaller than those of sulfur. All six axial positions are occupied by cyano ligands. The charge of the complex anion is 4−, which indicates that the oxidation

(11) (a) Mironov, Y. V.; Virovets, A. V.; Naumov, N. G.; Ikorskii, V. N.; Fedorov, V. E. *Chem.—Eur. J.* **2000**, *6*, 1361–1365. (b) Magliocchi, C.; Xie, X.; Hughbanks, T. *Inorg. Chem.* **2000**, *39*, 5000–5001. (c) Brylev, K. A.; Virovets, A. V.; Naumov, N. G.; Mironov, Y. V.; Fenske, D.; Fedorov, V. E. *Russ. Chem. Bull.* **2001**, *50*, 1140–1143. (d) Magliocchi, C.; Xie, X.; Hughbanks, T. *Inorg. Chem.* **2004**, *43*, 1902–1911.

(12) Naumov, N. G.; Cordier, S.; Perrin, C. *Solid State Sci.* **2003**, *5*, 1359–1367.

(13) Naumov, N. G.; Brylev, K. A.; Mironov, Y. V.; Virovets, A. V.; Fenske, D.; Fedorov, V. E. *Polyhedron* **2004**, *23*, 599–603.

(14) Naumov, N. G.; Artemkina, S. B.; Virovets, A. V.; Fedorov, V. E. *J. Solid State Chem.* **2000**, *153*, 195–204.

Table 2. Bond Distances (Å) and Angles (deg) of $(NMe_4)_4$[**1**]·$4H_2O$, $(NMe_4)_4$[**2**]·$2.67H_2O$, and $(PPh_4)_4$[**2**]·$2CH_3CN$[a]

	$(NMe_4)_4$[**1**]·$4H_2O$	$(NMe_4)_4$[**2**]·$2.67H_2O$	$(PPh_4)_4$[**2**]·$2CH_3CN$
Tc−Tc	2.5966(8)−2.598(1), av. 2.594(2)	2.626(2)−2.640(3), av. 2.63(1)	2.624(2)−2.638(2), av. 2.631(4)
Tc−Q	2.390(2)−2.403(2), av. 2.398(7)	2.506(2)−2.519(1), av. 2.51(1)	2.494(2)−2.509(2), av. 2.500(7)
Tc−C	2.115(9)−2.134(6), av. 2.12(1)	2.08(1)−2.17(1), av. 2.15(3)	2.11(1)−2.16(2), av. 2.13(3)
C−N	1.14(1)−1.16(1), av. 1.15(2)	0.99(2)−1.16(2), av. 1.10(6)	1.11(2)−1.16(2), av. 1.14(3)
Tc−Tc−Tc	59.78(2)−60.25(2), av. 60.00(7)	59.73(4)−60.29(4), av. 60.0(3)	59.78(4)−60.34(4), av. 60.0(1)
Tc−Tc−Tc	89.78(2)−90.22(2), av. 90.00(5)	89.79(4)−90.38(4), av. 90.0(2)	89.77(5)−90.23(5), av. 90.0(1)
Tc−Q−Tc	65.24(4)−65.81(5), av. 65.5(2)	63.03(5)−63.52(6), av. 63.3(3)	63.26(5)−63.79(5), av. 63.5(2)
Q−Tc−Q	89.51(6)−90.27(6), av. 89.82(2)	89.55(5)−90.48(6), av. 89.9(3)	89.47(5)−90.39(6), av. 89.9(2)
Q−Tc−Q	173.02(5)−173.36(6), av. 173.21(1)	175.51(6)−176.25(7), av. 175.9(3)	175.24(8)−176.20(5), av. 175.7(2)
Tc−C−N	177.8(8)−178.5(6), av. 178(1)	175(1)−179(1), av. 177(3)	177(1)−179(1), av. 178(2)

[a] Q = S for $(NMe_4)_4$[**1**]·$4H_2O$ and Se for $(NMe_4)_4$[**2**]·$2.67H_2O$ and $(PPh_4)_4$[**2**]·$2CH_3CN$.

Table 3. Calculated and Experimental Averaged Distances and C≡N Stretching IR Bands in $[Tc_6Q_8(CN)_6]^{4-}$ (Q = S, Se)

	M−M (Å)		M−Q (Å)		M−C (Å)		C≡N (Å)		C≡N stretching IR band/cm^{-1}	
	calcd	exp	calcd	exp	calcd	exp	calcd	exp	calcd	exp
$[Tc_6S_8(CN)_6]^{4-}$	2.639	2.594	2.491	2.398	2.103	2.12	1.20	1.15	2101	2114
$[Tc_6Se_8(CN)_6]^{4-}$	2.675	2.63	2.582	2.50, 2.51	2.106	2.13, 2.15	1.20	1.10, 1.14	2090	2105

state of all technetium ions is 3+. The Tc−Tc distances are av. 2.594(2) Å for $[\mathbf{1}]^{4-}$ and 2.63(1) Å for $[\mathbf{2}]^{4-}$. The Tc−Q distances are 2.398(7) Å for $[\mathbf{1}]^{4-}$ and 2.51(1) Å for $[\mathbf{2}]^{4-}$. These values are very similar to those of previously reported hexatechnetium clusters and the isoelectronic and isostructural hexarhenium and mixed rhenium−osmium complexes.[2b,c,m,6a,r,10b,c,e,15] The Tc−C bond distances of $[\mathbf{1}]^{4-}$ and $[\mathbf{2}]^{4-}$ are almost equal [av. 2.12(1) Å for $[\mathbf{1}]^{4-}$ and 2.15(3) Å for $[\mathbf{2}]^{4-}$] and similar to those of hexarhenium and mixed rhenium−osmium analogues.[6a,r,10b,c,e,15]

Electrochemical Properties. The cyclic voltammograms of $[\mathbf{1}]^{4-}$ and $[\mathbf{2}]^{4-}$ in a 0.1 M Bu_4NPF_6−CH_3CN solution are shown in Figure S4 in the Supporting Information. The new hexatechnetium(III) complexes $[\mathbf{1}]^{4-}$ and $[\mathbf{2}]^{4-}$ exhibit reversible one-electron-oxidation waves of Tc_6(24e/23e) at +0.99 and +0.74 V, respectively, vs Ag/AgCl. The one-electron redox wave of $[Tc_6S_8(CN)_6]^{4-}$ is +0.24 V more positive than that of $[Tc_6S_8Br_6]^{4-}$.[2m] This positive shift of the redox potential may be due to the difference between the π-electron-donating character of bromide and the π-electron-accepting character of cyanide. The $E_{1/2}$ value of Tc_6(24e/23e) for the new complexes is more positive in the case of sulfur than in the case of selenium, possibly because of the electronegativity of the face-capping chalcogenide. Chalcogenide-capped hexarhenium(III) cyanide in a 0.1 M Bu_4NPF_6−CH_3CN solution exhibited the Re_6(24e/23e) process at +0.60 V for $[Re_6S_8(CN)_6]^{4-}$ and +0.37 V for $[Re_6Se_8(CN)_6]^{4-}$.[3c] Therefore, the 24e valence state is thermodynamically more stable in the hexatechnetium complexes than in the hexarhenium analogues. This tendency was also observed in the M_6(24e/23e) process of the axial halide complexes $[M_6S_8X_6]^{4-}$ (M = Tc, Re; X = Br, I).[2m]

HOMO and LUMO Properties. The HOMO/LUMO levels, the frequencies of the C≡N stretching bands, and the electronic transition energies in $[Tc_6Q_8(CN)_6]^{4-}$ (Q = S, Se) were determined by DFT calculations using the *Gaussian 03* program at the B3LYP/LANL2DZ level. Table 3 shows the calculated and experimental geometrical parameters and the frequencies of the C≡N stretching bands of the hexatechnetium complexes. The calculated Tc−Tc, Tc−Q, and C≡N bond distances were slightly overestimated as compared to the experimental values (+0.04 Å for Tc−Tc, +0.07−0.09 Å for Tc−Q, and +0.05−0.1 Å for C≡N). The same tendency was also reported for the hexarhenium complexes.[5d,16] The calculated frequencies of the C≡N stretching bands for both sulfide- and selenide-capped hexatechnetium complexes are similar to the frequencies observed in the IR spectra. The calculated energies and components of the MOs near the frontier orbital levels for $[\mathbf{1}]^{4-}$ and $[\mathbf{2}]^{4-}$ are shown in Table 4. The energy and contour plots of the MOs near the frontier orbital levels for $[\mathbf{1}]^{4-}$ and $[\mathbf{2}]^{4-}$ are shown in Figure 3. The a_{2g} LUMO is localized on the technetium atoms (Tc, 100%) in both hexatechnetium complexes. The t_{1g} and t_{2u} orbitals, which have slightly higher energy than the LUMO, are mainly localized on the Tc_6Q_8 core (Tc, 70−76%; Q, 20−25%). The doubly degenerated e_g HOMOs are localized on the Tc_6Q_8 core (Tc, 70%; Q, 30%). The axial cyano ligands have a small effect on the HOMO and LUMO levels. In both Mulliken and NBO population analyses, the charge on the technetium atoms in the sulfide-capped complex is more positive than the charge on the technetium atoms in the selenide-capped complex (Mulliken analysis, −0.444 in $[\mathbf{1}]^{4-}$, −0.510 in $[\mathbf{2}]^{4-}$; NBO

Table 4. Calculated Energies and Components of MOs near the Frontier Orbital Levels for $[Tc_6Q_8(CN)_6]^{4-}$ (Q = S, Se)

		$[Tc_6S_8(CN)_6]^{4-}$				$[Tc_6Se_8(CN)_6]^{4-}$			
	sym	energy/eV	Tc	S	CN	energy/eV	Tc	Se	CN
LUMO+7,8	e_u	8.2	0.49	0.51	0	8.16	0.44	0.56	0
LUMO+4,5,6	t_{2u}	7.55	0.76	0.22	0.02	7.66	0.76	0.23	0.01
LUMO+1,2,3	t_{1g}	7.21	0.74	0.20	0.06	7.41	0.70	0.25	0.05
LUMO	a_{2g}	6.89	1.00	0	0	7.01	1.00	0	0
HOMO, HOMO−1	e_g	4.06	0.71	0.29	0	4.28	0.70	0.30	0
HOMO−2,3,4	t_{1u}	3.67	0.27	0.63	0.10	3.90	0.24	0.68	0.08
HOMO−5,6,7	t_{1g}	3.44	0.21	0.66	0.13	3.81	0.25	0.62	0.13
HOMO−8,9,10	t_{2u}	3.17	0.60	0.19	0.21	3.40	0.62	0.18	0.19

(15) Baudron, S. A.; Deluzet, A.; Boubekeur, K.; Batail, P. *Chem. Commun*. **2002**, 2124–2125.

(16) Kozlova, S. G.; Gabuda, S. P.; Brylev, K. A.; Mironov, Y. V.; Fedorov, V. E. *J. Phys. Chem. A* **2004**, *108*, 10565–10567.

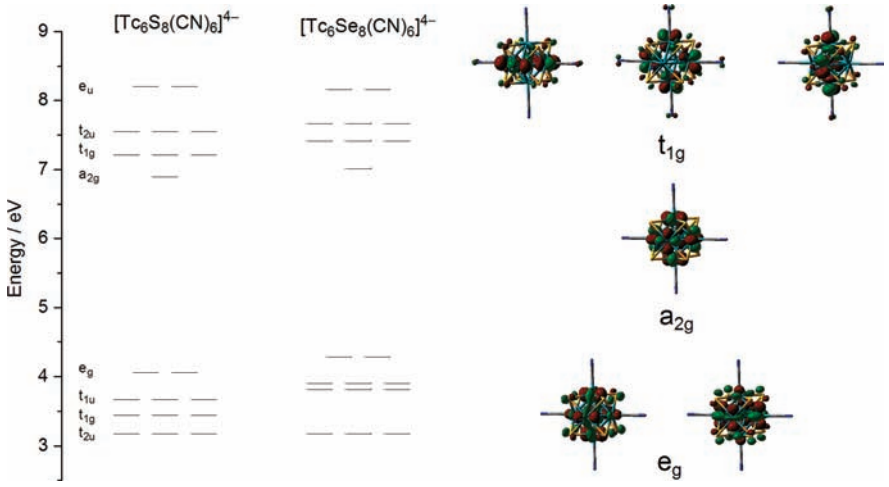

Figure 3. Energy diagrams near the HOMO/LUMO levels of $[Tc_6Q_8(CN)_6]^{4-}$ (Q = S, Se) and contour plots of the MOs near the frontier orbital levels of $[Tc_6S_8(CN)_6]^{4-}$.

analysis, −0.112 in $[\mathbf{1}]^{4-}$, −0.290 in $[\mathbf{2}]^{4-}$). Several studies have reported theoretical calculations of the electronic structure, electronic transition, and vibrational frequency of $[Re_6Q_8(CN)_6]^{4-}$ (Q = S, Se).[5d,16,17] It is worth pointing out that the components of the orbitals near the HOMOs and LUMOs in the Tc and Re complexes are very similar to each other although the energy levels are somewhat different.[18] The energy levels of HOMO and LUMO are stabilized in the order $[Tc_6S_8(CN)_6]^{4-}$ > $[Tc_6Se_8(CN)_6]^{4-}$ > $[Re_6S_8(CN)_6]^{4-}$ > $[Re_6Se_8(CN)_6]^{4-}$. Figure 4 shows a plot of the energy level of the HOMO in $[M_6Q_8(CN)_6]^{4-}$ (M = Tc, Re; Q = S, Se) against the redox potential of the M_6(24e/23e) process. The plot exhibits a good linear correlation with a slope value of −0.82 (r = 0.99). The M_6(24e/23e) redox potentials of M = Tc and Re clearly reflect the energy levels of the HOMO. It should be noted that the HOMO−LUMO energy gap of the hexatechnetium complexes is approximately 0.6 eV (4800 cm^{-1}) smaller than that of $[Re_6Q_8(CN)_6]^{4-}$ (HOMO−LUMO energy gap: 2.83 eV for $[\mathbf{1}]^{4-}$, 2.73 eV for $[\mathbf{2}]^{4-}$, 3.46 eV for $[Re_6S_8(CN)_6]^{4-}$, and 3.34 eV for $[Re_6Se_8(CN)_6]^{4-}$).

Electronic singlet transitions from the HOMO regions to the LUMO regions were also calculated using the TD-DFT method. The calculated and experimentally observed spectra for $[\mathbf{1}]^{4-}$ and $[\mathbf{2}]^{4-}$ are shown in Figures 5 and 6, respectively. The calculated excitation energies and oscillator strengths are summarized in Tables S1 and S2 in the Supporting Information. The TD-DFT calculations for both sulfide- and selenide-capped hexatechnetium complexes indicate that the substantially allowed singlet transitions in the range of 400−500 nm are ascribed to the Tc_6Q_8 core and that the major contribution is composed of $e_g \rightarrow t_{2u}$, $t_{2u} \rightarrow a_{2g}$, and $t_{1u} \rightarrow t_{1g}$ transitions. The values of the excitation energies with the largest oscillator strength [2.85 eV (437 nm) with 0.0036 for $[\mathbf{1}]^{4-}$ and

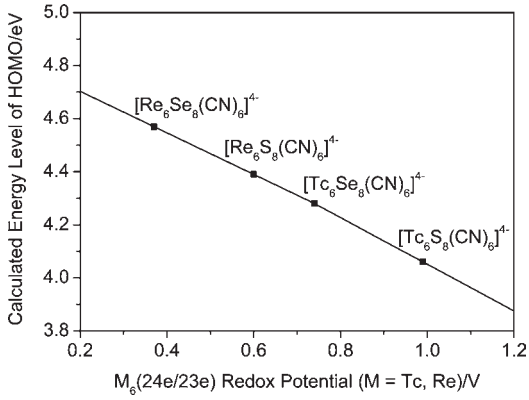

Figure 4. Plot of the energy level of the HOMO in $[M_6Q_8(CN)_6]^{4-}$ (M = Tc, Re; Q = S, Se) against the redox potential of the M_6(24e/23e) process.

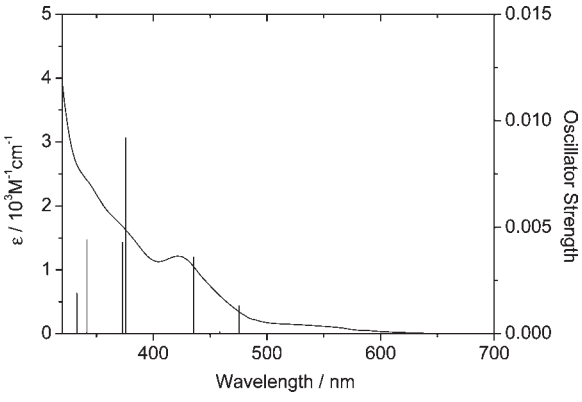

Figure 5. Experimental UV−vis spectrum for $(PPh_4)_4[Tc_6S_8(CN)_6]$ in acetonitrile at room temperature and calculated electronic transitions for $[Tc_6S_8(CN)_6]^{4-}$.

2.81 eV (441 nm) with 0.0031 for $[\mathbf{2}]^{4-}$] are similar to those of the observed absorption peak maximum energies [2.92 eV (425 nm) for $[\mathbf{1}]^{4-}$ and 2.80 eV (443 nm) for $[\mathbf{2}]^{4-}$]. The longer-wavelength shift of the selenide-capped complex at the lowest-energy electronic transition compared to that of the sulfide-capped complex in the hexatechnetium complex shows the same trend in the experimental UV−vis data in acetonitrile. In the case of the hexarhenium

(17) (a) Deluzet, A.; Duclusaud, H.; Sautet, P.; Borshch, S. A. *Inorg. Chem.* **2002**, *41*, 2537–2542. (b) Hernandez-acevedo, L.; Arratia-perez, R. *J. Chil. Chem. Soc.* **2003**, *48*, 125–128. (c) Baranovski, V. I.; Korolkov, D. V. *Polyhedron* **2004**, *23*, 1519–1526.

(18) We conducted DFT calculations on $[Re_6Q_8(CN)_6]^{4-}$ (Q = S, Se) following the same method as that used for the hexatechnetium complexes. The bond distances and angles in the optimized geometries of the rhenium complexes and the frequencies were in good agreement with the values calculated theoretically using the same basis set.

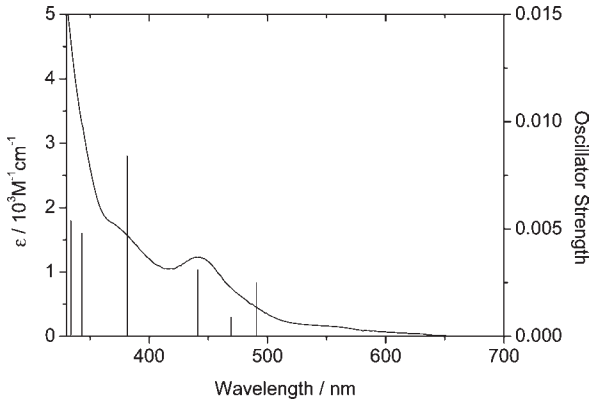

Figure 6. Experimental UV−vis spectrum for $(PPh_4)_4[Tc_6Se_8(CN)_6]$ in acetonitrile at room temperature and calculated electronic transitions for $[Tc_6Se_8(CN)_6]^{4-}$.

analogues, the substantially allowed lowest-energy transitions in our TD-DFT calculations are composed of the Re_6Q_8 core (major contribution: $e_g \rightarrow t_{2u}$, $t_{2u} \rightarrow a_{2g}$, and $t_{1u} \rightarrow t_{1g}$ transitions in the range of 360−410 nm; see the Supporting Information); thus, the electronic structure and electronic transition properties of $[Tc_6Q_8(CN)_6]^{4-}$ are similar to those of the hexarhenium analogues. On the basis of these facts, the hexatechnetium(III) cluster can be expected to exhibit photoluminenescence. Unfortunately, we were unable to detect photoluminescence in the chalcocyanide hexatechnetium complex by observation with the naked eye under a UV lamp at room temperature. The emission of $[Re_6Q_8(CN)_6]^{4-}$ was in the range of 600−1000 nm; the maximum emission wavelength values for Q = S, Se are 720−746 nm at 296 or 298 K in the solid state or solution.[3c,n,5a,d] The results of the DFT calculation indicate that the HOMO−LUMO energy gap of $[Tc_6Q_8(CN)_6]^{4-}$ is approximately 0.6 eV (4800 cm^{-1}) smaller than that of $[Re_6Q_8(CN)_6]^{4-}$. If such a difference between the emissive excited state and the ground state in energy exists in the hexatechnetium and hexarhenium complexes, the maximum emission wavelength value of the hexatechnetium complexes can be expected to be ca. 1100 nm.[19] Therefore, photoemission of the hexatechnetium complex might be shown in the near-IR region. An alternative interpretation is that the emission might be quenched by the vibration inducing nonradiative decay.

Conclusion

Discrete molecular sulfide- and selenide-capped hexatechnetium(III) clusters with axial cyano ligands $[Tc_6Q_8(CN)_6]^{4-}$ (Q = S, Se) were prepared from an octahedral hexatechnetium complex by depolymerization and axial ligand substitution, and the crystal structures of the complexes were determined. The redox potential of the Tc_6(24e/23e) process was more positive for the sulfide-capped complex than for the selenide-capped complex. DFT calculations of the octahedral hexatechnetium complexes revealed that the frequency of the calculated C≡N stretching band was similar to the observed frequency. It was found that the M_6(24e/23e) (M = Tc, Re) redox potential has a linear relationship with the energy of the HOMO level. It was also found that the electronic structures of the hexatechnetium and hexarhenium complexes are similar and that the hexatechnetium cluster complexes have a fairly small energy gap between the HOMO and LUMO. The smaller energy gaps observed for the hexatechnetium complexes might be related to the fact that the photoluminescence of the hexatechnetium(III) complexes could not be seen by the naked eye.

Acknowledgment. We thank Dr. K. Minato, Dr. Y. Shirasu, Dr. Y. Nagame, and Dr. I. Nishinaka of Japan Atomic Energy Research Agency for providing us with technetium metal for this study.

Supporting Information Available: Crystallographic data of $(NMe_4)_4$[**1**]·$4H_2O$, $(NMe_4)_4$[**2**]·$2.67H_2O$, and $(PPh_4)_4$[**2**]·$2CH_3CN$ in CIF format, tables of the calculated energies and components of MOs near the frontier orbital levels and of calculated excited-state energies, and figures of selected MOs and of calculated and observed absorption spectra. This material is available free of charge via the Internet at http://pubs.acs.org.

(19) Photoluminescence of the strong luminescent hexarhenium(III) complex $[Re_6S_8Cl_6]^{4-}$, with a maximum emission wavelength at 858 nm at 80 K in the solid state, could not be confirmed by the naked eye.